THE JOURNAL OF BIOLOGICAL CHEMISTRY VOL. 280, NO. 50, pp. 41777–41783, December 16, 2005

Effects of HMGN1 on Chromatin Structure and SWI/SNF-mediated Chromatin Remodeling*

Received for publication, September 1, 2005, and in revised form, October 20, 2005 Published, JBC Papers in Press, October 27, 2005, DOI 10.1074/jbc.M509637200

David A. Hill[‡1], **Craig L. Peterson**[§], **and Anthony N. Imbalzano**[‡]

From the [‡]*Department of Cell Biology at the University of Massachusetts Medical School, Worcester, Massachusetts 01655 and the* [§]*Program in Molecular Medicine at the University of Massachusetts Medical School, Worcester, Massachusetts 01605*

The dynamic modulation of chromatin structure is determined by many factors, including enzymes that modify the core histone proteins, enzymes that remodel the structure of chromatin, and factors that bind to genomic DNA to affect its structure. Previous work indicates that the nucleosome binding family of high mobility group proteins (HMGN) facilitates the formation of a chromatin structure that is more conducive for transcription. SWI/SNF complexes are ATP-dependent chromatin remodeling enzymes that alter nucleosome structure to facilitate the binding of various regulatory proteins to chromatin. Here we examine the structural consequences of reconstituting chromatin with HMGN1 and the resulting effects on hSWI/SNF function. We demonstrate that HMGN1 decreases the sedimentation velocity of nucleosomal arrays in low ionic strength buffers but has little effect on the structure of more highly folded arrays. We further demonstrate that HMGN1 does not affect SWI/SNF-dependent chromatin remodeling on either mononucleosomes or nucleosomal arrays, indicating that SWI/SNF functions independently of HMGN1.

The structure of chromatin is involved in the regulation of cellular processes that utilize the genome as a template, including transcription, replication, recombination, and repair. The structure of the nucleosome core particle containing 147 base pairs of DNA wrapped around an octamer of the four core histones has been solved (1), and recently the crystal structure of a tetranuclesome array has been obtained (2). Although the features of these static chromatin structures have been characterized to a high degree, the dynamic nature of chromatin makes it impossible to identify any one particular structure as the physiologically predominant form. Many factors contribute to the dynamic nature of chromatin, including enzymes that modify the core histones and enzymes that hydrolyze ATP to alter the structure of nucleosomes. In addition to chromatin-modifying enzymes, there are other chromatin-associated proteins that are involved in maintaining or altering chromatin structure, for example, linker histones, high mobility group (HMG)[2] chromatin proteins, and sequence-specific DNA binding regulatory proteins.

SWI/SNF chromatin remodeling enzymes are multisubunit complexes that hydrolyze ATP to alter chromatin structure to allow the binding of regulatory factors to nucleosomal DNA (3–6). SWI/SNF enzymes have been shown to both activate and repress a subset of genes in both yeast and mammals (7, 8). *In vitro* and *in vivo* evidence indicates that SWI/SNF enzymes can promote activator binding (3, 4, 9–11), TBP binding, and RNA polymerase II preinitiation complex formation and function (5, 12–15), as well as transcriptional elongation (16–18). The selectivity of SWI/SNF function at specific genes is most often explained via targeting by promoter bound regulatory proteins (19) and is supported by numerous examples of physical interactions between activators and repressors and different SWI/SNF subunits (7, 18, 20–27).

In addition to enzymatic processes that alter chromatin structure, there are non-histone chromatin proteins that interact with chromatin and possess the ability to alter its structure. The high mobility group proteins are just such a class of proteins and have been generally characterized as chromatin architectural proteins because of their ability to bind to and alter the structure of DNA (for reviews, see Refs. 28 and 29). There are three families of HMG proteins that are classified according to their functional DNA interaction motifs: HMGA, HMGB, and HMGN (30). The DNA binding motif for the HMGA family is called the "AT hook," the "HMG-box" defines the HMGB family, and the HMGN family is known for its nucleosome binding domain.

Members of the HMGN family include HMGN1, HMGN2, and HMGN3 (formerly known as HMG-14, HMG-17, and Trip 7, respectively) as well as a more recently described member, HMGN4 (31). Of the HMG proteins, only the HMGN family specifically interacts with the nucleosome core particle (32–35). Both HMGN1 and HMGN2 (hereafter referred collectively as HMGN1/N2) interact with the histones and the DNA of nucleosome cores and stabilize the nucleosomal DNA against nuclease digestion and thermal denaturation (32, 36–38).

Despite the stabilization effects that HMGN1/N2 proteins have on mononucleosomes and core particles, their structural contributions in chromatin fibers seems to be much different. In initial studies, HMGN1/N2 proteins were found to be enriched in transcriptionally active regions of chromatin, and HMGN1/N2-depleted chromatin became more sensitive to DNase I when reconstituted with purified HMGN1/N2, indicating that it could produce a more "open" structure as determined by DNase I sensitivity (39). Because of these data, HMGN1/N2 were thought to function *in vivo* as a factor that transforms transcriptionally repressive chromatin structure into an open structure more conducive for transcription initiation and/or elongation. The idea that HMGN1/N2 could unfold or otherwise alter repressive chromatin structure and promote transcription was an attractive model, and numerous subsequent studies reported that HMGN1/N2 does indeed enhance transcription initiation or elongation on chromatinized templates but not on naked DNA templates (40–46). One important observation is that enhancement of transcription was observed when HMGN1/N2 was added during the chromatin reconstitution process, but little or no effect was observed when added after reconstitution (41, 42, 44), indicating that HMGN1/N2 are functionally active when it is incorporated into chromatin at the time of assembly

* This work was supported by American Cancer Society Fellowship GMC-100065 (to D. A. H.) and by NCI/National Institutes of Health Grant P01 CA82834 (to A. N. I. and C. L. P.). The costs of publication of this article were defrayed in part by the payment of page charges. This article must therefore be hereby marked "*advertisement*" in accordance with 18 U.S.C. Section 1734 solely to indicate this fact.

[1] To whom correspondence should be addressed: Dept. of Cell Biology, S3-209, University of Massachusetts Medical School, 55 Lake Ave. North, Worcester, MA 01655. Tel.: 508-856-1049; Fax: 508-856-5612; E-mail: david.hill@umassmed.edu.

[2] The abbreviations used are: HMG, high mobility group; EMSA, electrophoretic mobility shifts assay.

but may not function properly if added after assembly. It is important to note that even though HMGN1/N2 has been shown to promote decompaction of chromatin structure, initial studies showed that these proteins did not prevent the formation of higher order chromatin structure (47). Thus, the *in vitro* evidence strongly supports the hypothesis that HMGN1/N2 contributes to a chromatin structure that is more transcriptionally competent; however, the precise structural contributions remain under investigation.

Because HMGN1/N2 protects nucleosomes from thermal denaturation and nuclease digestion in a manner similar to linker histone H1/H5 (48), it seems possible that they could also stabilize nucleosomes against SWI/SNF-mediated remodeling, as has been previously shown with linker histones (49–51). Conversely, because HMGN1/N2 has been shown to unfold chromatin into a transcriptionally competent structure, HMGN1 may promote SWI/SNF remodeling by presenting a chromatin structure that is more conducive to SWI/SNF activity or by stabilizing the structure following remodeling.

To distinguish between these possibilities, we assembled mononucleosomes without and with HMGN1 and subjected them to SWI/SNF remodeling assays. We show that nucleosomes assembled with HMGN1 are remodeled at the same rate as nucleosomes lacking HMGN1. Because we expected HMGN1 to either inhibit or promote the SWI/SNF reaction, we reasoned that any affect of HMGN1 might only be apparent on oligonucleosomal templates. We therefore assembled nucleosomal arrays without and with HMGN1 and characterized the effect that HMGN1 has on nucleosome array structure by analytical ultracentrifugation. Our data demonstrate that HMGN1 elongates arrays in low salt buffer as exhibited by a sedimentation velocity that is slower than that which is expected from HMGN1-containing arrays. Further analysis under conditions that promote $MgCl_2$-dependent chromatin folding reveals that HMGN1 does not affect the overall size or shape of the array. These characterized arrays were subsequently analyzed in SWI/SNF remodeling assays, and as observed for mononucleosomes, HMGN1 did not affect the rate of nucleosome remodeling, indicating that SWI/SNF activity is apparently unaffected by the interaction of HMGN1 with nucleosomal arrays.

MATERIALS AND METHODS

Protein Purification—HMGN1 was expressed from pETHMGN14 plasmid (gift from Dr. Ulla Hansen, Boston University) in BL21(DE3) and purified as described (44). HMGN1 was further purified from proteolytic products by resuspending the acetone washed pellet in 20 mM Tris-HCl pH 7.6, 300 mM NaCl and loading it onto a 1.5 × 15-cm P11 (Whatman) column equilibrated with the same buffer. HMGN1 was eluted with a 1-liter linear gradient from 0.3 to 1.0 M NaCl at a flow rate of 0.2 ml per min, and the peak fractions were identified by SDS-PAGE and pooled. Purified HMGN1 was submitted to the University of Massachusetts Medical School Laboratory for matrix-assisted laser desorption ionization mass spectroscopy analysis.

SDS Gels, Western Blots, and Antibodies—All SDS-polyacrylamide gels with HMGN1/N2 were either 15 or 18% acrylamide with a 39:1 ratio to bisacrylamide. Proteins were electroblotted overnight at 40 V in a tank at 4 °C to Protran BA 83 nitrocellulose. Nitrocellulose was blocked in 5% nonfat dry milk reconstituted in 1x TBST and was probed with antisera against HMGN1 that was diluted 1:1000. Secondary antibody was horseradish peroxidase-conjugated donkey anti-rabbit (Amersham Biosciences) diluted 1:4000 and was illuminated using ECL (Amersham Biosciences) or SuperSignal West Pico (Pierce). Polyclonal anti-HMGN1 antibody was generated by Covance by injecting a rabbit with cross-linked purified human recombinant HMGN1 protein. Cross-linking was carried out by incubating 1 mg of HMGN1 at 1:10 molar ratio with gluteraldehyde in 200 μl of 100 mM Tris-HCl, pH 7.6, for 1 h and stopping the reaction by adding L-lysine to 100 mM. Cross-linked HMGN1 was extensively dialyzed against 10 mM Tris-HCl, pH 7.6, before submission for immunization.

Nucleosome Core Particle, Nucleosome, Nucleosomal Array Assembly, and Characterization—Core particles were generated by digesting chicken erythrocytes nuclei with micrococcal nuclease (MNase) and isolating them as described (52). Nucleosomes were assembled as previously described (49) except that the 216-bp XP10 (gift from Jeffrey Hayes, University of Rochester) EcoRI to DdeI DNA fragment was not radiolabeled. Briefly, 2 μg of a purified XP10 EcoRI to DdeI fragment was mixed with chicken histone octamers at a 1:1 molar ratio in 50 μl of 10 mM Tris, pH 8, 250 μM EDTA with 2 M NaCl and was dialyzed to the same buffer with 2.5 mM NaCl over 16 h. HMGN1 was added to the nucleosomes at the point when the dialysis buffer reached 400 mM NaCl. Nucleosomal arrays were assembled with purified chicken octamers and a DNA template containing 11 head-to-tail repeats of the 208-bp 5 S rDNA sequence (208-11) (53). HMGN1 was incorporated into the arrays using a previously established protocol for reconstituting arrays with linker histones (54). Briefly, following nucleosomal array assembly the arrays were dialyzed into buffer containing 10 mM Tris-HCl, pH 8.0, 25 μM EDTA and 400 mM NaCl, adding the HMGN1 at various concentrations and dialyzing directly back into the same buffer having only 2.5 mM NaCl. Redialysis was performed on all arrays used in this study and had no effect on their gel migration properties or their distribution of sedimentation coefficients (data not shown). Analytical ultracentrifugation and nucleosome array folding assays were performed as previously described (55). Sedimentation data were generated in a Beckman analytical ultracentrifuge (XL-I), analyzed using UltraScan software, which employs the van Holde and Weishet method to remove the diffusion component (56), and plotted with Excel. The van Holde and Weishet method removes the diffusion component by taking advantage of the fact that sedimentation transport is proportional to the first power of time, whereas diffusional transport is proportional to the square root of time. The data are extrapolated in the limit of infinite time, which makes the contribution of diffusion on the boundary shape negligible (57).

Electrophoretic Mobility Shifts—Electrophoretic mobility shifts assays (EMSAs) with trimmed chicken core particles and purified HMGN1 were performed as described (32), with slight variation. 170 ng of core particles were incubated with varying amounts of HMGN1 in 10 μl of either 1.0 or 0.1 × TBE (TBE: 98 mM Tris, 98 mM boric acid, 1 mM EDTA), 5% glycerol for 5 min at room temperature. The mixture was loaded onto a 5% polyacrylamide gel and electrophoresed 100 V for 60 min in the same buffer. The gels were stained with ethidium bromide and visualized by UV. EMSAs of 208-11 nucleosomal arrays were accomplished by electrophoresing 200 ng of 208-11 nucleosomal array that had been assembled with or without HMGN1 in a buffer containing 20 mM Tris, 19 mM acetic acid, and 25 μM EDTA, 0.8 or 1.0% agarose gel at 100 V for 30–60 min. In experiments where 208-11 arrays ± HMGN1 were titrated with $MgCl_2$, individual aliquots were diluted 50:50 with the same buffer but containing 2× of the final concentration of $MgCl_2$ and incubated 10 min at room temperature. Glycerol was added to 5%, and the samples were electrophoresed as described above. As indicated in the text, some samples were centrifuged 17,000 × *g* for 30 min prior to loading onto the gel. Bands were visualized by staining the gel with ethidium bromide and illuminating with UV. Where indicated, the gel was electroblotted for Western analysis.

SWI/SNF Remodeling Assay— hSWI/SNF was purified as described previously from HeLa cells constitutively expressing FLAG-tagged Ini1 (58, 59). SWI/SNF remodeling activity on mononucleosomes was monitored using a restriction enzyme accessibility assay that has been described previously (49) with a variation in that the DNA was not radiolabeled. 400 fmol of nucleosomes were incubated in SWI/SNF reaction buffer (20 mM Tris-HCl, pH 7.6, 50 mM NaCl, 2.5 mM $MgCl_2$, 100 μg/ml bovine serum albumin, and 1 mM dithiothreitol) with 20 units of EcoRV restriction enzyme (New England Biolabs) and 185 fmol of SWI/SNF, and the reaction was started with the addition of ATP to 1 mM. Reactions were stopped at the indicated time points by vortexing 5-μl aliquots in a mixture of 10 μl TE with 10% glycerol and 10 μl of phenol chloroform isoamyl alcohol. Following centrifugation for 2 min at 17,000 × *g*, 10 μl of the supernatant was electrophoresed in a 1× TAE (40 mM Tris, 1 mM EDTA, 20 mM acetic acid), 5% polyacrylamide gel with 29:1 bisacrylamide ratio for 30 min at 10 V/cm. Digestion products were visualized by staining the gel with SYBR Green I (Molecular Probes) and quantified using ImageQuant software (Amersham Biosciences). The remodeling activity of hSWI/SNF on nucleosomal arrays was determined using a restriction enzyme accessability assay as previously described (53). 50 ng of 208-11 nucleosome array in 20 μl containing 20 mM Tris-HCl, pH 7.9, 1.5 mM $MgCl_2$, 50 mM NaCl, and 1 mM dithiothreitol was subjected to 10-min preincubation with 10 units of HincII (New England Biolabs) at room temperature. Following preincubation, 3 μl were removed for the zero time point, then 185 fmol of hSWI/SNF and 5 μl of 5 mM ATP were added and incubated for various amounts of time as indicated. Time points were taken by removing 5 μl and extracting it in a mixture of 10 μl TE containing 10% glycerol and 10 μl phenol chloroform isoamyl alcohol. Extracted DNA was electrophoresed for 30 min at 100 V on a 0.8% agarose 1× TAE gel containing SYBR Green I. The bands in the gel were visualized using an Alpha Imager and quantfied using ImageQuant software.

RESULTS

Human recombinant HMGN1 was expressed in BL21(DE3) and purified as described (44). Both SDS-PAGE (Fig. 1*A*) and mass spectroscopy (Fig. 1*B*) analysis of the purified HMGN1 indicated that it was homogenous with the correct molecular weight. One characteristic of HMGN proteins that distinguishes them from the other HMG proteins is the ability to bind to and form specific complexes with nucleosome core particles (32). The functionality and the concentration of our purified HMGN1 was tested in EMSA by titrating nucleosome core particles with increasing amounts of purified HMGN1 and electrophoresing the complexes in a 5% acrylamide gel made with either 1.0× or 0.1× TBE (Fig. 1). Previous work by others has demonstrated that two HMGN1 molecules bind to each core particle and that binding is cooperative under higher ionic strength conditions (32). Titration of core particles with HMGN1 in 0.1× TBE showed the formation of two distinct complexes (Fig. 1*C*, *lane 6*) culminating in a single discrete band at a 2:1 HMGN1 to core particle molar ratio. When the same titration was performed in 1× TBE, only one discrete shifted band formed (Fig. 1*D*, *lane 6*) as predicted (32). These data indicate that our purified HMGN1 protein behaves identically to those used in other studies.

One question we initially sought to answer was whether HMGN1 would stabilize the nucleosome in a way that would protect it from SWI/SNF remodeling or prevent SWI/SNF access to the nucleosome. SWI/SNF assays were performed on mononucleosomes assembled onto a well characterized 216-bp 5 S rDNA sequence from *Xenopus* borialis (60). This sequence has a unique EcoRV restriction site centrally located in the nucleosome positioning sequence, which is inaccessible

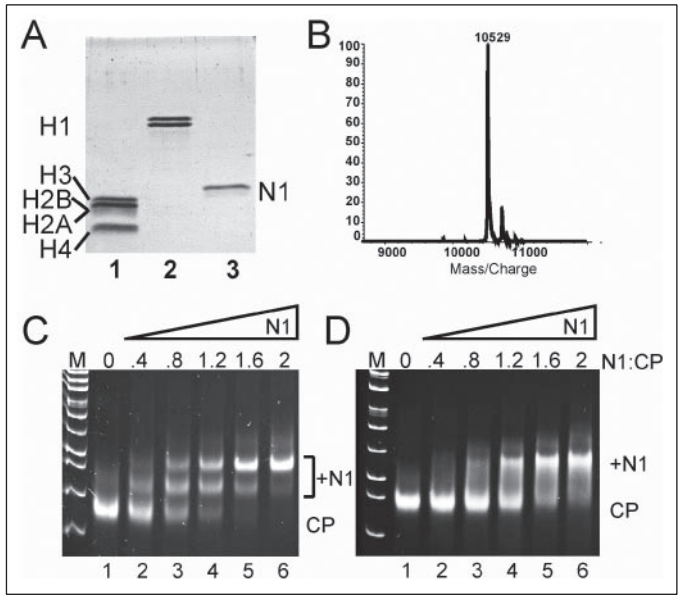

FIGURE 1. **Characterization of HMGN1.** *A*, SDS gel of chicken core histones (*lane 1*), linker histone H1 (*lane 2*), and purified recombinant HMGN1 (*lane 3*). *B*, mass spectroscopy analysis of the purified HMGN1. *C* and *D*, electrophoretic mobility shifts of nucleosome core particles titrated with increasing concentrations of purified HMGN1 in 5% acrylamide gels. Core particles and HMGN1 were incubated and electrophoresed in either 0.1× TBE (*C*) or 1.0× TBE (*D*). Molar ratios of HMGN1 to core particles were 0.0, 0.4, 0.8, 1.2, 1.6, and 2.0 in *lanes 1–6*, respectively.

to the restriction enzyme when the DNA is assembled into a nucleosome. The site becomes available for cleavage if the nucleosome undergoes remodeling and, when cleaved, generates restriction products one-half the size of the full-length DNA. We assembled nucleosomes without and with HMGN1 at molar ratios of 1 and 2 and used them as substrates in the enzyme accessibility assay (Fig. 2). To demonstrate that HMGN1 is incorporated into the nucleosome, an EMSA was performed using a 0.1× TBE gel. Nucleosomes assembled with HMGN1 have a retarded mobility when compared with the mobility of HMGN1-free nucleosomes (Fig. 2*A*). Results of the restriction enzyme accessibility assay indicated that the EcoRV site was readily cleaved in naked DNA (Fig. 2*B*) but was inaccessible when assembled into a nucleosome (Fig. 2*C*). When SWI/SNF and ATP were added to the reactions, the cleavage of the nucleosomal DNA was greatly enhanced, as demonstrated by the accumulation of cleavage products and a concomitant decrease in the amount of full-length nucleosomal DNA (Fig. 2*D*). HMGN1 assembled into nucleosomes at molar ratios of 1:1 or 2:1 did not affect the efficiency of template cleavage (Fig. 2, *E* and *F*). Independent experiments were quantified and plotted to demonstrate that there was no significant difference in the rate of remodeling between nucleosomes and HMGN1-containing nucleosomes (Fig. 2*G*). The graph contains plots showing that in the absence of SWI/SNF, HMGN1 alone did not affect the access of the restriction enzyme to its cleavage site on the nucleosome (Fig. 2*G*, *open squares* and *triangles*).

Because HMGN1 has been shown to affect the structure of longer chromatin templates, we were interested to know whether HMGN1 would affect SWI/SNF remodeling activity on nucleosomal arrays. Studies of chromatin structure and dynamics have been greatly facilitated through the use of specially designed DNA templates that can be assembled into chromatin arrays using purified components. In many cases these model DNA templates are made with 11–12 tandem head-to-tail repeats of the 5 S rDNA sequence (*e.g.* the 208-11 and 208-12 templates), which translationally positions nucleosomes (61, 62). Many aspects of chromatin structure, including the kinetics of assembly and

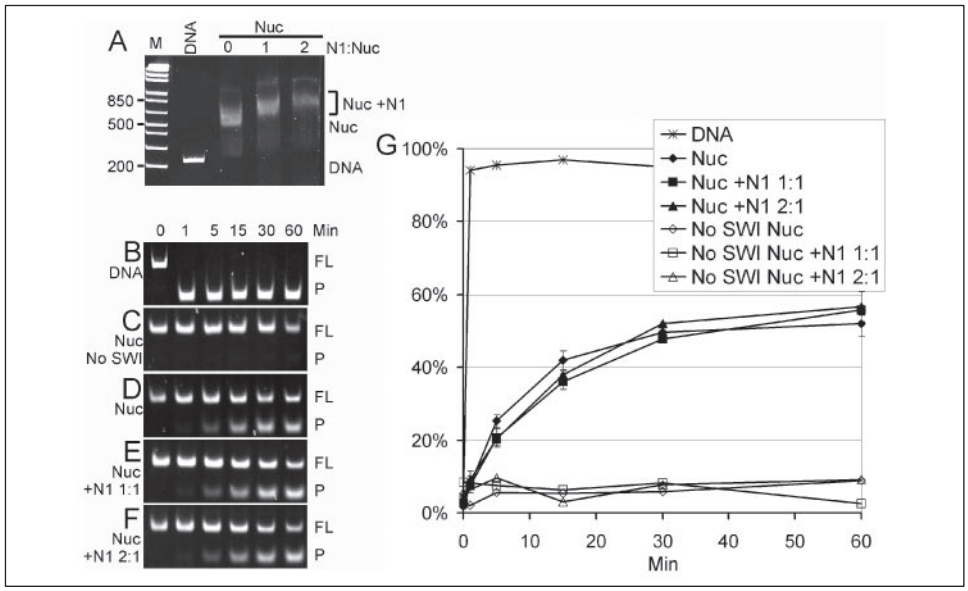

FIGURE 2. **SWI/SNF enzymes remodeling of HMGN1-containing nucleosomes.** *A*, nucleosomes assembled with HMGN1 to nucleosome ratios of 1 and 2 were electrophoresed on a 5% polyacrylamide gel to show a shift caused by the bound HMGN1. *B–F*, polyacrylamide gels were used to separate full-length (*FL*) and restriction products (*P*) from the restriction enzyme accessibility assay. Substrates were as follows: naked DNA (*B*), nucleosomes (no SWI/SNF) (*C*), nucleosomes (*D*), E & F) nucleosomes with HMGN1 at a 1:1 and 2:1 molar ratio to nucleosomes (*E* and *F*). *G*, quantification of the band intensities was graphed to show that the HMGN1-containing nucleosomes have the same remodeling rate as nucleosomes. Data with standard deviations are the average of three experiments.

salt-mediated folding, have been characterized using this system (63–65); however, the structural contributions of HMGN proteins on these arrays has not been investigated. Therefore, before performing the SWI/SNF remodeling assays, we first characterized the structure of this array system assembled with HMGN1.

Model 208-11 nucleosome arrays assembled in the presence of increasing amounts of HMGN1, up to 2 mol of HMGN1 per nucleosome, causes a stepwise shift in EMSAs (Fig. 3*A*). Titrations above molar ratios of 2 caused the shifted band to become more diffuse, indicating that oversaturation and nonspecific binding was occurring (data not shown). Western blot analysis of the EMSA gel demonstrated that HMGN1 migrated with the shifting 208-11 array band (Fig. 3*B*). Structural analyses of array folding are performed by incubating arrays in $MgCl_2$ (or higher concentrations of monovalent salt) and measuring the change in sedimentation velocity using analytical ultracentrifugation (64). To determine whether the conditions that promote array folding would disrupt or alter HMGN1 array binding properties, we performed the same titration of HMGN1 onto 208-11 arrays shown in Fig. 3*A* but in the presence of 1.5 mM $MgCl_2$ (Fig. 3*C*). The results clearly demonstrated that HMGN1 binds to the arrays and shifts them in the presence of $MgCl_2$ in a manner identical to what was observed in buffer without $MgCl_2$, thereby demonstrating that the presence of $MgCl_2$ did not affect binding of HMGN1 to the nucleosomal arrays. The Western blot of the titration gel shows that, as before, HMGN1 migrated with the shifted array (Fig. 3*D*).

One concern was that the addition of HMGN1 to nucleosomal arrays might cause extensive oligomerization or aggregation in the presence of $MgCl_2$, a phenomenon previously exhibited when linker histone H5 was assembled into nucleosomal arrays (66). To test this possibility, nucleosomal arrays without and with 2 mol of HMGN1 per nucleosome were incubated in buffer containing increasing amounts of $MgCl_2$, incubated for 15 min at room temperature, and then the samples were centrifuged at 17,000 × *g* for 30 min prior to agarose gel electrophoresis analysis (Fig. 3*E*). The HMGN1-containing arrays migrated more slowly in the gel than those without HMGN1, indicating that HMGN1 was still able to bind the arrays in buffer containing 2 mM $MgCl_2$. More importantly, the HMGN1-containing arrays did not aggregate, since bands were visible across the spectrum of the $MgCl_2$ titration (Fig. 3*E*, *lanes 5–8*) and because the optical density of the supernatant measured at 260 nm did not appreciably decrease (data not shown). Western blot analysis of the gel indicated that HMGN1 was present only in the array containing HMGN1 and that HMGN1 alone did not migrate as a discrete band with the same mobility as the arrays (Fig. 3*F*, *lane 9*).

Sedimentation velocity experiments in the analytical ultracentrifuge have been used to characterize the folding parameters of chromatin structure in solution. Structural characterization of the 208-11 array by sedimentation velocity analysis has shown that a 208-11 template fully saturated with nucleosomes sediments with a median sedimentation coefficient ($S_{20,w}$) of 29 in TE buffer (10 mM Tris, 25 μM EDTA) (53). This is in agreement with the analysis performed on the similar 208-12 array, which has been used extensively as a standard for nucleosome array folding studies and is the same sedimentation coefficient that is predicted for a fully extended "beads-on-a-string" conformation (67). Our reconstituted arrays displayed an average *S* of 30 (50% boundary fraction) with a nearly vertical curve, indicating that the sample was essentially homogeneous (Fig. 4*A*, *closed circles*). Arrays assembled with increasing amounts of HMGN1 (molar ratios of HMGN1 to nucleosome of 0.5, 1.0, 1.5, and 2.0 were analyzed, only data from 0, 1.0, and 2.0 are shown) had little effect on the average *S* value when sedimented in buffer without $MgCl_2$ (Fig. 4*A*). The Svedberg equation stipulates that the sedimentation coefficient is proportional to the mass of the particle and inversely proportional to the frictional coefficient. Addition of two HMGN1 proteins per nucleosome would add 8.4% to the mass of the array. Thus, this increase would dictate a 8.4% increase in *S* across all boundary fractions providing the binding of HMGN1 caused no structural change in the nucleosome array (66). However, the addition of HMGN1 increased the average *S* less than 2% across the boundary fractions (Fig. 4*A*). The simplest explanation for these results is that HMGN1 causes the array template to become slightly more elongated or less flexible, thus altering the frictional coefficient proportionally to the increase in mass. We do note, however, that the *S* values of HMGN1 containing arrays appear to diverge from *S* values of arrays lacking HMGN1 in the higher boundary fractions. This is likely caused by slight heterogeneity in the HMGN1-containing arrays.

When identical samples were incubated in buffer containing 1.5 mM $MgCl_2$, the average S changed from 30 S to over 40 S (Fig. 4*A*, compare *closed circles* with *open circles*), indicating that the arrays folded into a more compact structure as observed previously (64). As with other nucleosomal arrays sedimented under similar conditions, the curves are no longer vertical but reach higher *S* values in the upper boundary

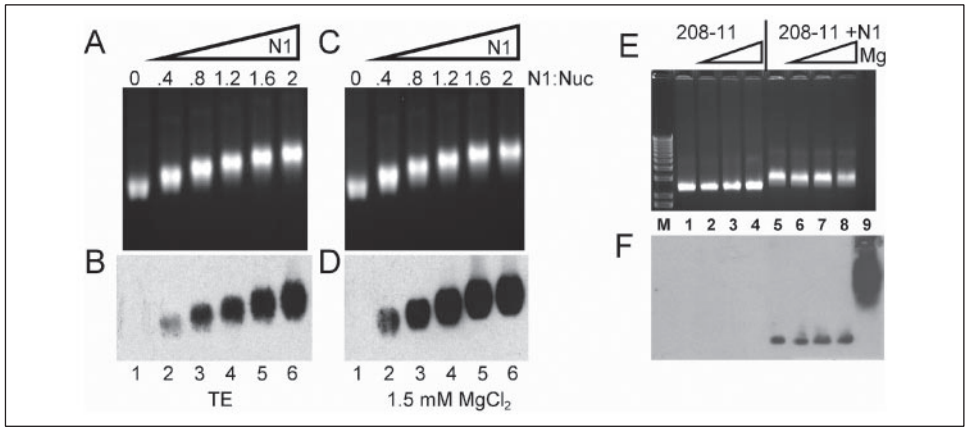

FIGURE 3. **Characterization of 208-11 on nucleosomal arrays assembled with HMGN1.** *A*, electrophoretic mobility shifts of 208-11 array assembled with increasing amounts of HMGN1. Molar ratios of HMGN1 to nucleosomes were 0, 0.4, 0.8, 1.2, 1.6, and 2.0 in *lanes 1–6*, respectively. Arrays were incubated in buffer without $MgCl_2$ (*A*) or in buffer with 1.5 mM $MgCl_2$ (*C*), for 30 min prior to electrophoresis in a 0.8% agarose 1× TAE gels. Gels were electroblotted to nitrocellulose and probed with α-HMGN1 (*B* and *D*). E) 208-11 arrays without (*lanes 1–4*) and with HMGN1 at molar a ratio of 2 (*lanes 5–8*) were incubated in buffer containing 0, 1.5, 1.75, and 2 mM $MgCl_2$ (*lanes 3–5* and *7–9*, respectively) for 30 min, centrifuged for 30 min at 17,000 × *g*, and electrophoresed on 0.8% agarose gel. *F*, Western blot of the gel in *E* probed with α-HMGN1 antibody. *Lane 9* was loaded with only purified HMGN1.

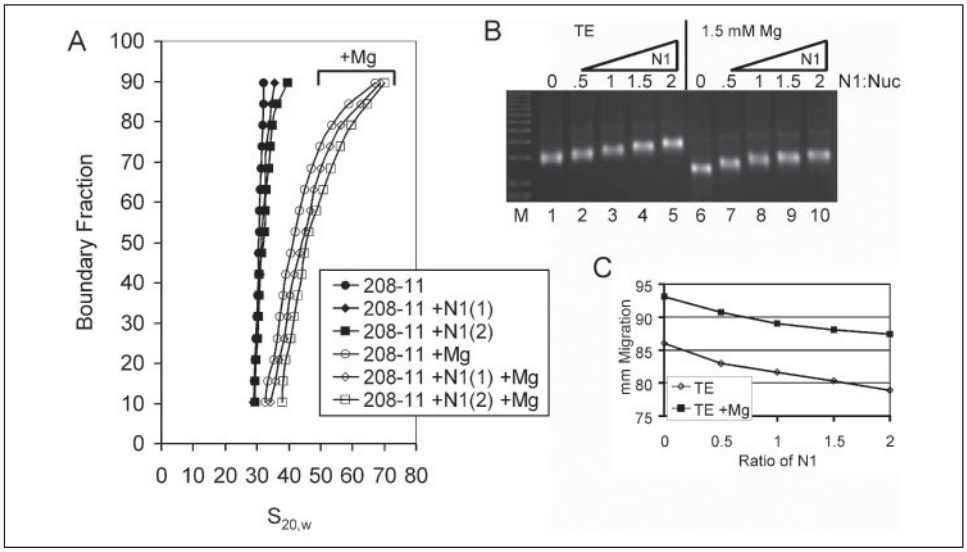

FIGURE 4. **Sedimentation velocity analysis of 208-11 arrays.** *A*, sedimentation velocity analysis of arrays in buffer without $MgCl_2$ (*solid symbols*) or with 1.5 mM $MgCl_2$ (*open symbols*) titrated with increasing concentrations of HMGN1. Molar ratios of HMGN1 to nucleosomes was 0.0 (*circles*), 1.0 (*diamonds*), or 2.0 (*squares*) (for clarity, data for HMGN1 at ratios of 0.5 and 1.5 are not shown). *B*, EMSA of samples recovered from the analytical ultracentrifuge and electrophoresed in a 0.8% agarose gel. Molar ratios of HMGN1 to nucleosomes were 0, 0.5, 1.0, 1.5, and 2.0 in *lanes 1–5* and *6–10*, respectively. *C*, plot of the relative migration distances from the well of bands in *B*; arrays were incubated in buffer without $MgCl_2$ (*diamonds*) or with 1.5 mM $MgCl_2$ (*squares*).

fractions. This curve is typical of molecules that adopt structures that are in equilibrium between larger and more slowly sedimenting (lower boundary fractions) and smaller structures that sediment more quickly (higher boundary fractions). Because all of our samples have a component that reaches 55 S, a value predicted for the structure of the 30-nm fiber, we conclude that the conditions employed here folds arrays into the maximally folded state, which are in equilibrium with more elongated, slower migrating species.

In contrast to the samples sedimented in buffer without $MgCl_2$, the samples sedimented in $MgCl_2$ showed a clear stepwise increase in S with increasing amounts of HMGN1 across the entire boundary fraction. The stepwise increase in sedimentation velocity in buffer containing $MgCl_2$ corresponds precisely to the expected value predicted due to the additional mass of HMGN1. Furthermore, the curves are parallel to each other, indicating that across the entire boundary fraction, the *S* value increased to the same extent. We interpret this to mean that HMGN1 has little effect on altering the structure of a compact, folded chromatin array.

To demonstrate that the samples retained HMGN1 during the sedimentation velocity experiment, the samples were recovered from the sample cell of the analytical ultracentrifuge and electrophoresed side-by-side in an agarose gel (Fig. 4*B*). The stepwise mobility shift indicates that HMGN1 remained bound to the arrays incubated in buffers without and with $MgCl_2$. One noticeable feature made more apparent from plotting the migration distances of the bands in the gel presented in Fig. 4*B* is that the arrays incubated in $MgCl_2$ migrated more rapidly than the arrays incubated in buffer without $MgCl_2$ (Fig. 4*C*), thus confirming the sedimentation results showing that arrays incubated in $MgCl_2$ are more compact.

To measure the nucleosome remodeling activity of SWI/SNF on arrays containing HMGN1, arrays characterized by analytical ultracentrifugation were recovered from the centrifuge and subjected to a restriction enzyme accessibility assay. The 208-11 array template was designed with a unique SalI restriction site in the central nucleosome that is protected from nuclease digestion by a positioned nucleosome. This site becomes accessible through nucleosome remodeling by SWI/SNF and related enzymes (53). Like the mononucleosome SWI/SNF assay, the activity of chromatin remodeling is measured by comparing a decrease in band intensity of the full-length array DNA with a concomitant increase in the cleavage product, which is one-half of the original array DNA length. The results of the SWI/SNF assay clearly showed that the accessibility of the SalI site in the arrays containing no HMGN1 (Fig. 5*A*) was identical to the arrays containing HMGN1 at a molar ratio of 2 (Fig. 5*B*). Plotting the results of SWI/SNF assays from all the assembled arrays previously analyzed in the analytical ultracentrifuge demonstrated that HMGN1 did not affect the remodeling activity of SWI/SNF on nucleosomal arrays (Fig. 5*C*) and suggests that SWI/SNF functions independently of HMGN1. Furthermore, HMGN1-containing arrays were refractory to restriction enzyme cleavage in the absence of ATP, indicating that HMGN1 alone does not expose the restriction site for digestion.

In summary, we sought to determine whether HMGN1 would have

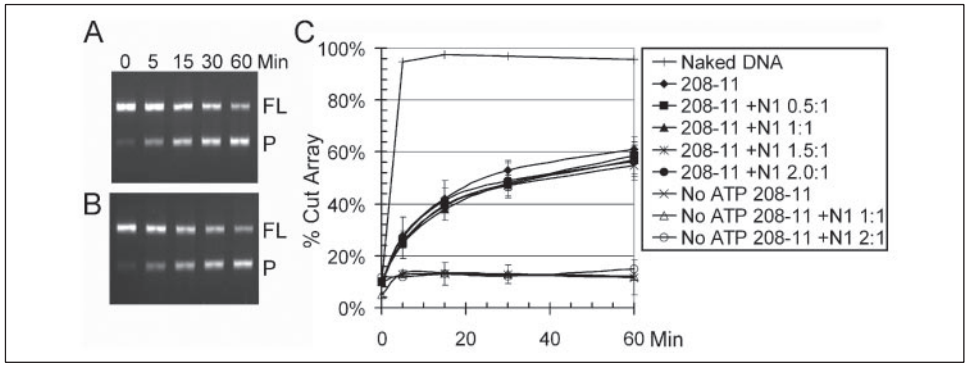

FIGURE 5. **SWI/SNF nucleosome remodeling assay on arrays containing HMGN1.** 208-11 arrays recovered from the analytical ultracentrifuge were subjected to a SWI/SNF-dependent restriction enzyme accessibility assay. The resulting full-length (*FL*) and digested products (*P*) were separated in a 0.8% agarose gel. Arrays assembled without (*A*) or with increasing amounts of HMGN1 up to a molar ratio of HMGN1 to nucleosome of 2.0 (*B*) were assayed. *C*, graph of the percent increase in digested product from three independent assays at all concentrations of HMGN1.

an effect on SWI/SNF-mediated nucleosome remodeling. We clearly demonstrate that HMGN1 does not affect the rate of SWI/SNF-dependent nucleosome remodeling when assembled into mononucleosomes or nucleosomal arrays. Our study further characterized the structural contributions that HMGN1 has on chromatin arrays assembled with purified components. The data indicate that HMGN1 has no detectable effect on the structure of compact chromatin fibers as analyzed by ultracentrifugation but that it does elongate or stiffen extended chromatin structures.

DISCUSSION

We set out to test whether HMGN1 would promote or inhibit SWI/SNF nucleosome remodeling activity. We reasoned that if HMGN1 bound to the nucleosome it might inhibit SWI/SNF chromatin remodeling activity, much like binding of linker histones H1/H5 inhibited SWI/SNF function (49–51). On the other hand, if HMGN1 unfolds chromatin structure to promote transcription, we thought that it might also promote SWI/SNF remodeling by unfolding arrays to present a chromatin structure that is more conducive to SWI/SNF remodeling. Our data demonstrate that neither hypothesis is true. HMGN1, unlike linker histone H1/H5, does not affect the rate of SWI/SNF remodeling activity on nucleosomes or nucleosomal arrays. Our results, if extrapolated to *in vivo* systems, suggest that SWI/SNF enzymes can function without a need to first remove HMGN1 from chromatin. Furthermore, our data clearly demonstrate that HMGN1 does not promote SWI/SNF remodeling activity on chromatin arrays *in vitro*. Hence, it seems likely that HMGN1 and SWI/SNF function independently from one another *in vivo*.

HMGN1 and linker histone H1 share several nucleosome preservation characteristics. For example, they both protect nucleosomes against thermal denaturation and nucleolytic digestion. Although H1 has been shown to inhibit SWI/SNF remodeling on both nucleosomes and arrays (49–51), our data clearly demonstrate that HMGN1 does not affect that ability of SWI/SNF to remodel nucleosomes or nucleosomal arrays. Possible explanations for the difference could be attributed to where these proteins bind the nucleosome. While both linker histones and HMGN1 have been modeled to interact with nucleosomal DNA, linker histones are modeled to interact with the DNA near the dyad axis of symmetry (68), whereas HMGN1 is modeled to interact with nucleosomal DNA further into the nucleosome away from the DNA exit and entry points (69).

The structure of chromatin plays an important role in regulating cellular processes, but the exact contribution of HMGN1 to chromatin structure is not well defined. Our studies on the structure of nucleosomal arrays assembled with purified components indicate that HMGN1 affects array chromatin structure only under conditions that produce an extended beads-on-a-string structure. Our data indicate that the sedimentation velocity of the 208-11 array in buffers lacking $MgCl_2$ is changed very little when increasing amounts of HMGN1 are incorporated into the array. Because we did not observe an increase in *S* with the addition of HMGN1 in low salt buffer, it can be assumed that the frictional coefficient increased proportionally to the mass due to increasing HMGN1 content in the arrays. To account for these findings, we concluded that HMGN1 is most likely increasing the frictional coefficient by slightly elongating or by reducing the flexibility of the chromatin filament. We have no reason to believe that HMGN1 is displacing the core histone tails to achieve this observation. To rule out this possibility, sedimentation analysis would have to be conducted on arrays assembled with tailless core histones. The caveat to this experiment is that HMGN1 has been reported not to interact with nucleosomes which have had their core histone tails removed by trypsinization (38).

Transcription assays on closed circular mini-chromosomes have been used to demonstrate that HMGN1 increases the rate of transcription on chromatin templates but not on naked DNA (40–46). Characterization of the effects of HMGN1 on the structure of mini-chromosomes has been assayed using micrococcal nuclease digestion, restriction enzyme accessability, and sucrose gradient sedimentation. The sucrose gradient sedimentation analyses of SV40 or M13 minichromosomes, assembled i*n vivo* or in *Xenopus laevis* extracts containing 3 mM $MgCl_2$, respectively, demonstrated that arrays assembled with HMGN1 migrated more slowly than those lacking HMGN1. These results were interpreted to mean that minichromosomes assembled with HMGN1 have a less compact structure (42, 44). In contrast to these previous studies, however, our data using arrays assembled with purified components and quantitative titrations of HMGN1 onto a well defined chromatin template indicate that HMGN1 has little effect on compact chromatin structure formed in buffer containing $MgCl_2$. One potential difference may be that HMGN1 behaves differently on closed circular templates than on linear arrays. Alternatively, in light of our results, it seems possible that HMGN1 may confer to individual nucleosomes a structure that allows the transcription machinery to function more efficiently rather than affecting the global structure of the chromatin array.

Acknowledgments—We thank Dr. Ulla Hansen (Boston University) for the pETHMG-14 vector and Dr. Peter Horn and Kimberly Crowley (University of Massachusetts Medical School) for assistance with operation and data acquisition of the Beckman analytical ultracentrifuge. We thank Drs. Walter Hill (University of Montana) and Borries Demeler (University of Texas Health Science Center, San Antonio, TX) for helpful discussion.

REFERENCES

1. Luger, K., Mader, A. W., Richmond, R. K., Sargent, D. F., and Richmond, T. J. (1997) *Nature* **389,** 251–260

2. Schalch, T., Duda, S., Sargent, D. F., and Richmond, T. J. (2005) *Nature* **436,** 138–141
3. Côté, J., Quinn, J., Workman, J. L., and Peterson, C. L. (1994) *Science* **265,** 53–60
4. Kwon, H., Imbalzano, A. N., Khavari, P. A., Kingston, R. E., and Green, M. R. (1994) *Nature* **370,** 477–481
5. Imbalzano, A. N., Kwon, H., Green, M. R., and Kingston, R. E. (1994) *Nature* **370,** 481–485
6. Wang, W., Xue, Y., Zhou, S., Kuo, A., Cairns, B. R., and Crabtree, G. R. (1996) *Genes Dev.* **10,** 2117–2130
7. Martens, J. H., Verlaan, M., Kalkhoven, E., and Zantema, A. (2003) *Mol. Cell. Biol.* **23,** 1808–1816
8. Sif, S. (2004) *J. Cell. Biochem.* **91,** 1087–1098
9. de la Serna, I. L., Ohkawa, Y., Berkes, C. A., Bergstrom, D. A., Dacwag, C. S., Tapscott, S. J., and Imbalzano, A. N. (2005) *Mol. Cell. Biol.* **25,** 3997–4009
10. Burns, L. G., and Peterson, C. L. (1997) *Mol. Cell. Biol.* **17,** 4811–4819
11. Cosma, M. P., Tanaka, T., and Nasmyth, K. (1999) *Cell* **97,** 299–311
12. Soutoglou, E., and Talianidis, I. (2002) *Science* **295,** 1901–1904
13. Lomvardas, S., and Thanos, D. (2001) *Cell* **106,** 685–696
14. Salma, N., Xiao, H., Mueller, E., and Imbalzano, A. N. (2004) *Mol. Cell. Biol.* **24,** 4651–4663
15. Ryan, M. P., Jones, R., and Morse, R. H. (1998) *Mol. Cell. Biol.* **18,** 1774–1782
16. Davie, J. K., and Kane, C. M. (2000) *Mol. Cell. Biol.* **20,** 5960–5973
17. Brown, S. A., Imbalzano, A. N., and Kingston, R. E. (1996) *Genes Dev.* **10,** 1479–1490
18. Corey, L. L., Weirich, C. S., Benjamin, I. J., and Kingston, R. E. (2003) *Genes Dev.* **17,** 1392–1401
19. Cosma, M. P. (2002) *Mol. Cell* **10,** 227–236
20. Cheng, S. W., Davies, K. P., Yung, E., Beltran, R. J., Yu, J., and Kalpana, G. V. (1999) *Nat. Genet.* **22,** 102–105
21. Fryer, C. J., and Archer, T. K. (1998) *Nature* **393,** 88–91
22. Kadam, S., McAlpine, G. S., Phelan, M. L., Kingston, R. E., Jones, K. A., and Emerson, B. M. (2000) *Genes Dev.* **14,** 2441–2451
23. Kowenz-Leutz, E., and Leutz, A. (1999) *Mol. Cell* **4,** 735–743
24. Liu, H., Kang, H., Liu, R., Chen, X., and Zhao, K. (2002) *Mol. Cell. Biol.* **22,** 6471–6479
25. Ma, Z., Chang, M. J., Shah, R., Adamski, J., Zhao, X., and Benveniste, E. N. (2004) *J. Biol. Chem.* **279,** 46326–46334
26. Magenta, A., Cenciarelli, C., De Santa, F., Fuschi, P., Martelli, F., Caruso, M., and Felsani, A. (2003) *Mol. Cell. Biol.* **23,** 2893–2906
27. Roberts, C. W., and Orkin, S. H. (2004) *Nat. Rev. Cancer* **4,** 133–142
28. Bustin, M., Lehn, D. A., and Landsman, D. (1990) *Biochim. Biophys. Acta* **1049,** 231–243
29. Bustin, M., and Reeves, R. (1996) *Prog. Nucleic Acids Res. Mol. Biol.* **54,** 35–100
30. Bustin, M. (2001) *Trends Biochem. Sci.* **26,** 152–153
31. Birger, Y., Ito, Y., West, K. L., Landsman, D., and Bustin, M. (2001) *DNA Cell Biol.* **20,** 257–264
32. Sandeen, G., Wood, W. I., and Felsenfeld, G. (1980) *Nucleic Acids Res.* **8,** 3757–3778
33. Mardian, J. K., Paton, A. E., Bunick, G. J., and Olins, D. E. (1980) *Science* **209,** 1534–1536
34. Albright, S. C., Wiseman, J. M., Lange, R. A., and Garrard, W. T. (1980) *J. Biol. Chem.* **255,** 3673–3684
35. Shirakawa, H., Herrera, J. E., Bustin, M., and Postnikov, Y. (2000) *J. Biol. Chem.* **275,** 37937–37944
36. Paton, A. E., Wilkinson-Singley, E., and Olins, D. E. (1983) *J. Biol. Chem.* **258,** 13221–13229
37. Gonzalez, P. J., and Palacian, E. (1990) *J. Biol. Chem.* **265,** 8225–8229
38. Crippa, M. P., Alfonso, P. J., and Bustin, M. (1992) *J. Mol. Biol.* **228,** 442–449
39. Weisbrod, S. T. (1982) *Nucleic Acids Res.* **10,** 2017–2042
40. Trieschmann, L., Postnikov, Y. V., Rickers, A., and Bustin, M. (1995) *Mol. Cell. Biol.* **15,** 6663–6669
41. Crippa, M. P., Trieschmann, L., Alfonso, P. J., Wolffe, A. P., and Bustin, M. (1993) *EMBO J.* **12,** 3855–3864
42. Trieschmann, L., Alfonso, P. J., Crippa, M. P., Wolffe, A. P., and Bustin, M. (1995) *EMBO J.* **14,** 1478–1489
43. Weigmann, N., Trieschmann, L., and Bustin, M. (1997) *DNA Cell Biol.* **16,** 1207–1216
44. Ding, H. F., Bustin, M., and Hansen, U. (1997) *Mol. Cell. Biol.* **17,** 5843–5855
45. Ding, H. F., Rimsky, S., Batson, S. C., Bustin, M., and Hansen, U. (1994) *Science* **265,** 796–799
46. Paranjape, S. M., Krumm, A., and Kadonaga, J. T. (1995) *Genes Dev.* **9,** 1978–1991
47. McGhee, J. D., Rau, D. C., and Felsenfeld, G. (1982) *Nucleic Acids Res.* **10,** 2007–2016
48. Lindsey, G. G., and Thompson, P. (1989) *Biochim. Biophys. Acta* **1009,** 257–263
49. Hill, D. A., and Imbalzano, A. N. (2000) *Biochemistry* **39,** 11649–11656
50. Horn, P. J., Carruthers, L. M., Logie, C., Hill, D. A., Solomon, M. J., Wade, P. A., Imbalzano, A. N., Hansen, J. C., and Peterson, C. L. (2002) *Nat. Struct. Biol.* **9,** 263–267
51. Ramachandran, A., Omar, M., Cheslock, P., and Schnitzler, G. R. (2003) *J. Biol. Chem.* **278,** 48590–48601
52. Libertini, L. J., and Small, E. W. (1980) *Nucleic Acids Res.* **8,** 3517–3534
53. Logie, C., and Peterson, C. L. (1997) *EMBO J.* **16,** 6772–6782
54. Howe, L., Iskandar, M., and Ausio, J. (1998) *J. Biol. Chem.* **273,** 11625–11629
55. Carruthers, L. M., and Hansen, J. C. (2000) *J. Biol. Chem.* **275,** 37285–37290
56. van Holde, K., and Weischet, W. O. (1978) *Biopolymers* **17,** 1387–1403
57. Demeler, B., Saber, H., and Hansen, J. C. (1997) *Biophys. J.* **72,** 397–407
58. Schnitzler, G., Sif, S., and Kingston, R. E. (1998) *Cell* **94,** 17–27
59. Sif, S., Stukenberg, P. T., Kirschner, M. W., and Kingston, R. E. (1998) *Genes Dev.* **12,** 2842–2851
60. Hayes, J. J., and Wolffe, A. P. (1992) *Proc. Natl. Acad. Sci. U. S. A.* **89,** 1229–1233
61. Simpson, R. T., Thoma, F., and Brubaker, J. M. (1985) *Cell* **42,** 799–808
62. Simpson, R. T., and Stafford, D. W. (1983) *Proc. Natl. Acad. Sci. U. S. A.* **80,** 51–55
63. Hansen, J. C., van Holde, K. E., and Lohr, D. (1991) *J. Biol. Chem.* **266,** 4276–4282
64. Schwarz, P. M., and Hansen, J. C. (1994) *J. Biol. Chem.* **269,** 16284–16289
65. Fletcher, T. M., and Hansen, J. C. (1996) *Crit. Rev. Eukaryotic Gene Expression* **6,** 149–188
66. Carruthers, L. M., Bednar, J., Woodcock, C. L., and Hansen, J. C. (1998) *Biochemistry* **37,** 14776–14787
67. Hansen, J. C., Ausio, J., Stanik, V. H., and van Holde, K. E. (1989) *Biochemistry* **28,** 9129–9136
68. Hayes, J. J., Pruss, D., and Wolffe, A. P. (1994) *Proc. Natl. Acad. Sci. U. S. A.* **91,** 7817–7821
69. Alfonso, P. J., Crippa, M. P., Hayes, J. J., and Bustin, M. (1994) *J. Mol. Biol.* **236,** 189–198

Effects of HMGN1 on Chromatin Structure and SWI/SNF-mediated Chromatin Remodeling

David A. Hill, Craig L. Peterson and Anthony N. Imbalzano

J. Biol. Chem. 2005, 280:41777-41783.
doi: 10.1074/jbc.M509637200 originally published online October 27, 2005
